ARTICLE
Journal of Cellular Biochemistry 115:1206–1216 (2014)

Journal of Cellular Biochemistry

# Vinculin Regulates Assembly of Talin: β3 Integrin Complexes

Suman Yadav Nanda,[1]* Thuy Hoang,[1] Priya Patel,[1] and Hao Zhang[2]

[1]*Department of Biological Chemistry, Johns Hopkins School of Medicine, Baltimore, MD 21205, USA*

[2]*Department of Molecular Microbiology and Immunology, Bloomberg School of Public Health, Baltimore, MD 21205, USA*

## ABSTRACT

Vinculin is a talin-binding protein that promotes integrin-mediated cell adhesion, but the mechanisms are not understood. Because talin is a direct activator of integrins, we asked whether and how vinculin regulates the formation of integrin: talin complexes. We report that VD1 (aa 1-258) and its talin-binding mutant, VD1A50I, bind directly and equally to several β integrin cytoplasmic tails (βCT). Results from competition assays show that VD1, but not VD1A50I, inhibits the interaction of talin (Tn) and talin rod (TnR), but not talin head (TnH) with β3CT. The inhibition observed could be the result of VD1 binding to one or more of the 11 vinculin binding sites (VBSs) in the TnR domain. Our studies demonstrate that VD1 binding to amino acids 482-911, a VBS rich region, in TnR perturbs the interaction of rod with β3CT. The integrin activation assays done using CHOA5 cells show that activated vinculin enhances αIIbβ3 integrin activation and that the effect is dependent on talin. The TnR domain however shows no integrin activation unlike TnH that shows enhanced integrin activation. The overall results indicate that activated vinculin promotes talin-mediated integrin activation by binding to accessible VBSs in TnR and thus displacing the TnR from the β3 subunit. The study presented, defines a novel direct interaction of VD1 with β3CT and provides an attractive explanation for vinculin's ability to potentiate integrin-mediated cell adhesion through directly binding to both TnR and the integrin cytoplasmic tail. J. Cell. Biochem. 115: 1206–1216, 2014. 

**KEY WORDS:** VINCULIN; INTEGRIN ACTIVATION; TALIN; BETA-CYTOPLASMIC TAILS

Integrins are a family of transmembrane heterodimeric proteins, composed of α and β subunits, each with a relatively small cytoplasmic tail. Integrins mediate cell adhesion to extracellular matrix proteins, which is a master regulatory event required for cell survival, differentiation, and migration [Hynes, 2002]. Among integrins, β1 is the most ubiquitously expressed subunit and associates with a number of α subunits resulting in distinct heterodimers with diverse functions. The two major isoforms of β1 integrin are β1 A, expressed most ubiquitously, except in the red blood cells (RBCs) and the β1D, specifically expressed in the junctional structures of striated muscles [Bozyczko et al., 1989]. The RBCs express mainly αIIbβ3, which also expressed in platelets and is largely responsible for their aggregation. Integrin αIIbβ3 is involved in maintaining hemostasis and its activation is very tightly regulated by both the external ligands and intracellular signaling [Leisner et al., 2007]. Thus making it a very good model system to understand and elucidate the mechanisms by which particular intracellular proteins regulate integrin mediated cell adhesion.

The intracellular proteins that co-localize with integrins at focal adhesions, vinculin [Xu et al., 1998; Gallant et al., 2005] and talin (Tn) [Priddle et al., 1998] have long been known to promote integrin mediated cell adhesion to extracellular matrix. Much is known about how talin promotes integrin-mediated adhesion. Talin, composed of a head domain (TnH) linked by a short unstructured region to an extended rod domain (TnR), determines integrin affinity/avidity for extracellular ligands by direct interaction with the cytoplasmic tail of the β subunit [Calderwood et al., 1999; Wegener et al., 2007 Anthis et al., 2009]. The TnR has a second integrin binding subdomain, IBS2 [Moes et al., 2007; Rodius et al., 2008], that does not activate integrin [Tremuth et al., 2004]. The available evidence suggests that IBS2 links integrin-talin complexes to the cytoskeleton [Moes et al., 2007]. TnR also contains a conserved actin binding site

Conflict of interest: The authors state that there are no conflicts of interest.

Grant sponsor: NIH grant; Grant number: GM41605.

*Correspondence to: Dr. Suman Yadav Nanda, Department of Biological Chemistry, Johns Hopkins School of Medicine, Baltimore, MD 21205, USA. E-mail: sumanynanda@gmail.com

Manuscript Received: 10 December 2013; Manuscript Accepted: 17 January 2014

Accepted manuscript online in Wiley Online Library (wileyonlinelibrary.com): 20 January 2014

DOI 10.1002/jcb.24772 • © 2014 Wiley Periodicals, Inc.

[McCann and Craig, 1997], 11 cryptic vinculin binding sites (VBSs) [Papagrigoriou et al., 2004; Gingras et al., 2005], and a dimerization helix [Smith and McCann, 2007]. Biochemical and cellular studies suggest that integrin binding sites are masked in full-length talin by interdomain TnH and TnR interactions [Goksoy et al., 2008; Banno et al., 2012]. Thus the talin head-rod interaction likely regulates talin-mediated integrin activation.

In contrast to talin, much less is known about how vinculin promotes integrin mediated cell adhesion. Structurally, vinculin is organized into a head domain (Vh) connected by an unstructured proline-rich region to an actin-binding tail domain, Vt. Vh is itself composed of 4 subdomains, VD1-4, of which VD1 binds talin. An intramolecular interaction between VD1, VD4, and Vt constrains vinculin in a strongly autoinhibited conformation [Johnson and Craig, 1994; Cohen et al., 2005]. Autoinhibited vinculin forms no detectable complex with talin or filamentous actin as determined by in vitro binding assays with soluble proteins and by assays in living cells [Johnson and Craig, 1995; Chen et al., 2006; Cohen et al., 2006]. In cells, autoinhibited vinculin is localized predominantly in the cytosol whereas in focal adhesions, vinculin is detected in either in its open/active actin-binding conformation, or in mostly closed conformation [Chen et al., 2005]. In its activated conformation, or as separated domains, vinculin has the ability to interact with both talin, Kd $\sim 10^{-7}$ M [Cohen et al., 2006], and F-actin, Kd $\sim 10^{-6}$ M [Bakolitsa et al., 1999]. Several sets of data suggest that vinculin exerts its effects on adhesion by providing additional bridging of integrin talin complexes to the actin cytoskeleton [Humphries et al., 2007]. Two recent publications present evidence for participation of vinculin in integrin activation in cells, as assayed by binding of antibodies specific for activated integrin [Nolz et al., 2007; Ohmori et al., 2010]. Another study provides evidence that activated vinculin induces clustering of activated form of integrins [Humphries et al., 2007]. All these studies show that the effect of vinculin is dependent on talin, shown either by talin knockdown [Ohmori et al., 2010] or by use of a talin non-binding vinculin mutant [Humphries et al., 2007].

In the present study, we have used in vitro biochemistry, protein mutagenesis, and live cell integrin activation assays to ask whether the interaction of vinculin with talin regulates the ability of talin to bind and activate integrin αIIbβ3.

## MATERIALS AND METHODS

### ANTIBODIES

Primary antibodies were PAC-1, ligand-mimetic monoclonal IgM antibody that detects activated αIIbβ3 [Abrams et al., 1994] (Becton Dickinson); A2A9/6 mouse monoclonal to detect total αIIbβ3 [Bennett et al., 1983] (Santa Cruz sc 21783L); mouse monoclonal anti-vinculin VinG-11 (Santa Cruz Biotechnology sc-55465); affinity-purified rabbit polyclonal anti-EGFP. Secondary antibodies were Cy5 donkey anti-mouse IgG (Jackson ImmunoResearch #715-175-1500); DyLight 649 AffiniPure donkey anti-mouse IgM (Jackson Immuno Research #715-495-020); IRDye$^{TM}$ 680 donkey anti-mouse IgG (DaMIgG680); IRDye$^{TM}$ 800CW donkey anti-rabbit IgG (DaRIgG800) (LI-COR # 926-32222 and #926-32213, respectively). Fatty acid and globulin free BSA was from Sigma, # A0281.

### cDNA CONSTRUCTS

Construction of pEGFPC1/human talin has been described [Cohen et al., 2006]. The multiple cloning site (MCS) of pEGFPC1 was modified to introduce an EcoRV site to facilitate the subcloning of TnR from pET30a/human talin rod (TnR; aa 397-2541), a gift from Dr. Stephen Lam), using EcoRV and EcoRI. Talin head (TnH; 1-435aa) was subcloned from pECFPC1/TnH (gift of Dr. Wherle-Haller) into pEGFPC1, using XhoI and EcoRI sites. Drs. David Critchley and Armando del Rio gifted pET151TOPO/TnR482-911 construct. IBS2 1975-2293 was subcloned in pET15b using NdeI and BamHI sites. The following constructs expressing chicken vinculin have been described: pEGFPC1/V1-1066 (wild-type or A50I); pEGFPC1/V1-851 (Vh) wild-type or A50I mutation; pEGFPC1/V1-1066 bearing T12 or D4 autoinhibition mutations; pET15b-YFP-VD1; pET15b VD1 (wt or A50I) [ Cohen et al., 2005; Chen et al., 2006]. pET15b-heptad repeat-β3 integrin cytoplasmic model tail cDNA [Pfaff et al., 1998] was the gift of Dr. Mark Ginsberg. We obtained codon optimized sequences for bacterial expression of human β1 A and β1D integrin tails from GenScript and cloned them into pET15b using HindIII and BamHI sites in modified pET15b heptad-repeat β3 construct to produce 6His-heptad repeat-β1 A/β1D cytoplasmic tail proteins. As a negative control, the cytoplasmic tail of αIIb was subcloned from Homo sapiens integrin αIIb cDNA (GenBank: BC117443.1) using HindIII and BamHI sites in modified pET15b-heptad repeat-β3 construct. The mutants of pET15b-β3 construct were made using the Stratagene Quickchange mutagenesis kit.

### PROTEIN EXPRESSION AND PURIFICATION

Recombinant 6His-tagged VD1 (aa 1-258), 6His-VD1A50I, 6His-IBS2, and 6His-TEV-TnR 482-911 were expressed in *Escherichia coli* and purified from extracts by Ni-NTA (nickel- nitrilotriacetic acid) affinity chromatography. 6His-YFP-VD1 was prepared as described [Cohen et al., 2005]. His-tags were removed using biotinylated thrombin and then incubated with immobilized streptavidin beads to remove the thrombin (Novagen). His-tag from TnR 482-911 was removed using 6His-TEV protease (gift from Dr. Erin Goley) in the reaction buffer (50 mM TrisCl pH8.0, 0.5 mM EDTA, 1 mM DTT) at 16 °C for 14–16 h. Cleaved TnR 482-911 was incubated with NTA beads to remove the cleaved His tag and the TEV protease. Cleaved proteins were dialyzed extensively versus Fusion Protein Storage (FPS) buffer +1 mM EDTA (10 mM Tris, pH 7.5, 100 mM NaCl, 0.02% azide), and then FPS only, supplemented with protease inhibitor cocktails I & II (PICs I & II). Dialyzed proteins were snap frozen in liquid nitrogen and stored at −80 °C. For YFP-tagged proteins, storage was at −80 °C after dialysis vs. 50% glycerol in FPS. Integrin cytoplasmic tail constructs were expressed in BL21(DE3) cells (Novagen) and purified by Ni-affinity chromatography followed by reverse phase C18 high performance liquid chromatography column [Lad et al., 2007]. The concentration of purified proteins was measured using the BioRad-Protein assay with a BSA standard or by absorption at 280 nm using a NanoDrop spectrophotometer and calculated extinction coefficients.

### CELL CULTURE, TRANSFECTION, AND LYSATE PREPARATION

$2–3 \times 10^6$ HEK 293 cells were cultured on 0.1% gelatin-coated 10 cm tissue culture plates in high glucose DMEM (MediaTech) supplemented with 10% FCS (Fetal calf serum) in a 5% $CO_2$ incubator at 37 °C. Cells were transfected with EGFP vinculin and talin constructs using LipofectAMINE/Plus reagent (Invitrogen) as described [Cohen et al., 2005]. HEK cells were detached by trypsinization 48–72 h after transfection and washed 2× with calcium and magnesium-free Dulbecco's PBS (CMF-DPBS). Pellets were resuspended in 500 μl/plate of cold cell lysis buffer (0.74× CMF-DPBS, 10 mM Imidazole, 0.1% TritonX 100, 5 mM β-ME, 2 mM $MgCl_2$, 0.2 mM EGTA, 2× PICs I & II). The cell suspensions were incubated for 10 min on ice and then centrifuged at 16,000×*g* for 30 min at 4 °C.

CHOA5 cells stably expressing human αIIbβ3 integrin [Zaffran et al., 2000] (gift from Dr. Joan Fox) were propagated in DMEM:F12 (Mediatech, Inc. Cat.# 10-092-CV) with 10% fetal calf serum. For transfection, $3.5 \times 10^6$ cells were plated on 0.1% gelatin-coated 10 cm tissue culture plates. Cells were transfected the next day at 70–80% confluency using LipofectAMINE/Plus reagent. Transfection efficiencies ranged from 50 to 80%. Cells were analyzed for integrin activation 48 h after transfection, by flow cytometry.

### PREPARATION OF INTEGRIN TAIL AFFINITY MATRIX AND DIRECT BINDING ASSAYS

Purified β1D, β1A, and β3-cytoplasmic tails were adsorbed to the Ni-NTA beads as described [Lad et al., 2007] with modifications as follows. The beads were resuspended in assay buffer (0.74× CMF-Dulbecco's PBS, 10 mM Imidazole, 0.1% TritonX, 5 mM β-ME, and 2 mM $MgCl_2$, pH 7.6, containing protease inhibitor cocktails. Purified and thrombin cleaved VD1 (5 μM) was incubated with 25 μl of 10% (v/v) suspension of cytoplasmic tail-coupled NTA resin, overnight at different temperatures, 4, 25, and 37 °C. Total reaction volume was 200 μl. After centrifugation, the supernatant was removed and the beads were washed 2× in the assay buffer. Protein pulled down by the beads was loaded on 4–12% Bis-Tris SDS NuPAGE gels and analyzed after staining with Coomassie Blue formaldehyde stain.

### DETERMINATION OF BINDING ISOTHERM FOR INTEGRIN β3 CYTOPLASMIC TAIL AND PURIFIED VD1

For estimating the binding constants different concentration of β3 integrin cytoplasmic tail proteins (0.5–40 μM) were loaded onto NTA resin as described [Lad et al., 2007]. Purified and thrombin cleaved 100 nM YFP-VD1 (wild-type or A50I) was incubated with 25 μl of 10% (v/v) suspension of 6His-β3-coated NTA resin, 16–20 h at 37 °C in assay buffer. After centrifugation, the fluorescence of unbound YFP-VD1/A50I in the supernatant was assayed on the fluorimeter (Jobin Yvon). YFP was excited at 490 nm, and peak emission at 527 nm was observed using 2-mm excitation and 2-mm emission slit widths. To check the integrity of constructs during the course of reaction, the bead pull downs were analyzed on 4–12% Bis-Tris SDS NuPAGE.

### SUPERNATANT DEPLETION BINDING ASSAYS

Purified β3 cytoplasmic tail was coupled on the Ni-NTA beads as described above. HEK293 cell lysates expressing EGFP-talin constructs (~100 nM) were incubated with 25 μl of 10% (v/v) suspension of β3-coupled NTA resin, overnight at 37 °C in presence or absence of thrombin cleaved 5 μM VD1 (wt or A50I). After centrifugation, the fluorescence of unbound talin constructs in the supernatant was assayed with a Fluoromax-3 spectrofluorimeter (HORIBA Jobin Yvon) at 22 °C. EGFP emission was recorded at 510 nm with excitation at 480 nm. The integration time was 0.2 s. The excitation and emission slit widths were 3 and 5 mm, respectively. Protein pulled down by the beads was loaded on 4–12% Bis-Tris SDS NuPAGE and blotted onto nitrocellulose membrane (BioRad laboratories). The proteins were detected using primary antibodies against EGFP and His-tag. Primary antibodies were detected with DaRIgG800 and DaMIgG680 using the Odyssey infrared imaging system (LI-COR Biotechnology). For competition studies using this assay, the competitor was added at the same time as the other reactants.

### INTEGRIN αIIbβ3 ACTIVATION ASSAY

The assay was performed according to the detailed protocol found in [Bunch, 2010]. In brief, transfected CHO A5 cells were trypsinized, washed in DMEM:F12 + 10% serum, and then washed in modified Tyrodes (12.1 mM $NaHCO_3$, 5 mM HEPES, 137 mM NaCl, 2.6 mM KCl, 5.6 mM glucose, 1 mg/ml fatty acid free BSA, pH 7.3). Cells ($3–5 \times 10^5$) were suspended in 50 μl of Tyrode's buffer supplemented with 1.0 mM Ca/Mg in presence or absence of 1 mM $Mn^{2+}$ or in Tyrode's buffer supplemented with 1.0 mM EDTA. $Mn^{2+}$ activates integrin directly by displacing a regulatory calcium ion in the extracellular domain and is the positive control for total activation competent αIIbβ3 [Ni et al., 1998]. EDTA disrupts ligand binding sites on integrin and is the control for non-specific binding of PAC1 antibody [Abrams et al., 1994]. Cells ($3–5 \times 10^5$) were incubated with 0.5 μg PAC1/50 μl reaction, to measure activated αIIbβ3 or 0.5 μg A2A9/50 μl reaction to measure total αIIbβ3 for 25 min at room temperature. Cells were washed in cold modified Tyrode's and incubated with appropriate secondary antibodies DyLight 647 RaMIgM (for PAC1) and Cy5DaMIgG (for A2A9/6) for 25 min on ice. The cells were also incubated with secondary antibody alone as a control for any non-specific staining.

The samples were analyzed by flow cytometry. Data were acquired on a MoFlo cytometer (Beckman Coulter, Miami, FL, USA) using software Summit version 4.0. The GFP was excited by a 488 nm Coherent Enterprise II 621 laser with power regulation at 100 mW. The GFP emission signal was collected from a PMT behind an attenuation filter (ND 1.0) and a 510/30 band pass filter with PMT voltage setting at 500 V. The DyLight 647 and Cy5 fluorochromes were excited with 35 mV 633 nm HeNe Laser (Melles Groit). The emission signals were collected from a 670/30 nm band pass filter with PMT voltage setting at 640 V. All samples were run and analyzed with constant PMT voltage settings. Quadrant cursor was set based on negative controls. Dead cells (propidium iodide positive), debris, cell doublets, and aggregates were excluded from analysis.

### CALCULATION OF αIIbβ3 ACTIVATION

The effect of expressing various constructs in CHOA5 cells was seen both in the percentage of PAC1 binding cells and in the mean

fluorescence intensity (MFI) of the PAC1 binding population. Therefore, to estimate integrin activation, the percent of cells in the PAC1+ EGFP+ quadrant (R3 on the flow cytometry graphs) was multiplied by the MFI of that population. Non-specific binding of PAC1 was calculated in the same manner from the EDTA treated samples and subtracted from the previous value. Results were normalized to PAC1 binding on cells expressing EGFP only (activation index = 1). The enhanced integrin activation for the constructs was assessed using one-tailed *t*-test against the GFP activation index value. The percent of cells expressing integrin αIIbβ3 as detected by monoclonal antibody A2A9, did not vary between constructs by more than 5% and was ~80% of the total cells. Parallel samples were treated with $Mn^{2+}$ to verify the presence of activation competent integrin. To verify expression of the constructs, cell lysates were assessed by immuno-blot.

### STATISTICS

The effect of VD1 on talin constructs binding to integrin tail was assessed using two-tailed *t*-tests. We used GraphPad Prism 5 (GraphPad software) and excel graphs for statistical analysis. The error bars in the figures are expressed as mean ± SEM. All *P* values $<0.05$ were considered significant.

## RESULTS

### THE VD1 DOMAIN BINDS DIRECTLY TO SEVERAL β INTEGRIN CYTOPLASMIC TAILS

To determine the binding of VD1 (aa 1-258) to β3CT we used an in vitro pull down assay. As control we also tested the binding to other integrin cytoplasmic tail constructs, αIIb, β1A, and β1D. VD1 showed varied binding to the different cytoplasmic tails and little or no binding was observed with unconjugated NTA resin and with αIIb matrix (Fig.1). The temperature-dependence of the interactions indicates that specific binding observed at 4 °C got significantly improved at physiological temp 37 °C. As a positive control for the pull down assay, we analyzed the binding of EGFP tagged talin constructs, Tn, TnH, and TnR from lysates to these integrin tails (Fig. S1 of Supporting Information). The results show that specific binding of talin constructs to integrin cytoplasmic tails was also significantly improved at 37 °C.

### CHARACTERIZATION OF THE DIRECT VD1: β3 INTERACTION

Structural studies show that β3 [Ulmer et al., 2001 Wegener et al., 2007] has a propensity to form amphipathic helices in its membrane proximal (MP) region, suggesting that VD1 might bind to β integrins by a mechanism similar to that used by VD1 to bind VBSs in talin [Gingras et al., 2005]. To test this idea, we assayed VD1A50I, a point mutation that occludes the VBS binding groove between two helices of VD1 [Izard et al., 2004]. Analysis of VD1A50I binding to β3 shows that it binds specifically and to the same extent as wildtype VD1 (Fig. 2A). Binding capacities of VD1 and VD1A50I were compared using purified YFP-VD1, YFP-VD1A50I and varying the concentration of coupled β3 on NTA beads. The immobilized β3 binds to both VD1 molecules to the same extent, as shown by the similar Kd values (Fig. 2B). However, the affinity constants could not be obtained accurately by varying purified VD1 concentrations because VD1 self-associates at high concentrations. Thus, we conclude that β3 do not bind to VD1 via the talin binding groove.

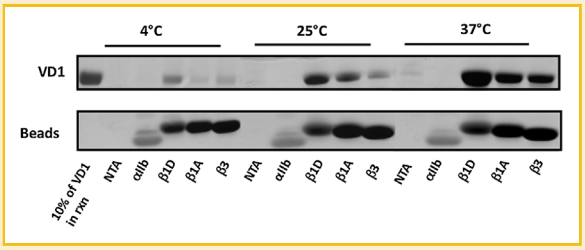


Fig. 1. VD1 binds directly and specifically to β integrin cytoplasmic tail proteins. The cytoplasmic tails of β1A, β3, β1D, or αIIb integrin, adsorbed to NTA beads as described in Materials and Methods, were used to pull down purified and thrombin cleaved VD1 domain. An SDS PAGE analysis was performed to assess the direct binding of VD1 with different integrin cytoplasmic tails. VD1 binding to NTA beads alone and αIIb coupled on beads were taken as negative controls. First lane shows 10% of the VD1 in reaction and the subsequent lanes show the increased binding of VD1 to β1D, β1A, and β3 cytoplasmic tails with increasing temperature.

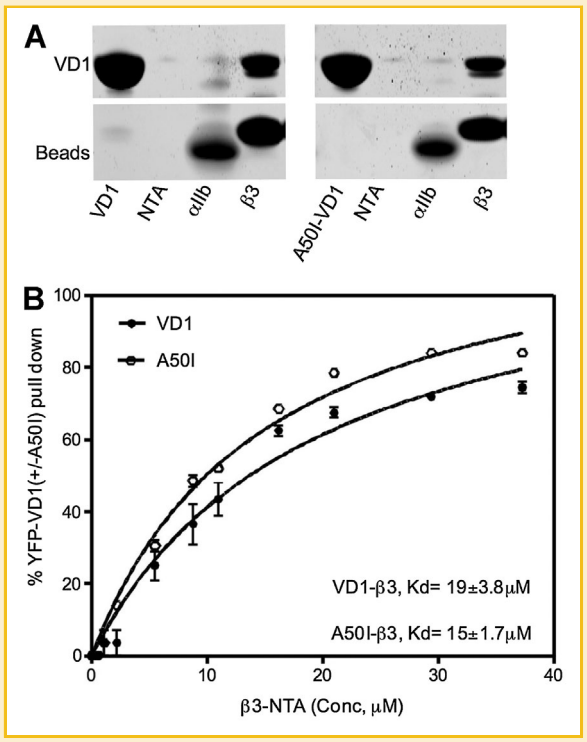


Fig. 2. VD1 and the VD1A50I talin-binding mutant show similar binding to β3 cytoplasmic tail. (A) The binding specificity of VD1 (wt or A50I) to β3 cytoplasmic tail was analyzed on 4–12% SDS-PAGE. (B) The binding of Tc-YFP-VD1 (wt or A50I) to different concentrations of β3 integrin cytoplasmic tail (0.5–37 μM) coupled to NTA beads was plotted using the GraphPad Prism software. The results for VD1 (filled circles) and VD1A50I (open circles) are plotted (n = 2).

### EFFECT OF VD1 ON Tn, TnR, TnH BINDING TO β3 CYTOLPASMIC TAIL

Talin, specifically TnH, has been identified as a direct activator of integrins [Calderwood et al., 1999; Tadokoro et al., 2003] and vinculin has been suggested to enhance talin-dependent integrin activation [Nolz et al., 2007; Ohmori et al., 2010]. To gain insight on how vinculin regulates integrin activation, we assayed for an effect of VD1 on the interaction of EGFP-Tn, TnH, and TnR with β3CT, in vitro. The HEK 293 cells lysate expressing EGFP tagged Tn constructs were pull down using β3-NTA matrix in presence and absence of VD1 (wt or A50I). We found that VD1 inhibits Tn and TnR interaction, but has no effect on TnH construct, which lacks VD1-binding site (Fig. 3A,B). The talin-binding mutant, VD1A50I, has no effect on binding of any talin construct to β3, further confirming that the inhibitory effect requires that VD1 bind talin (Fig. 3A,B). The gel analysis (Fig. 3B) shows that the constructs remained intact under the assay conditions.

Dose-response analysis shows that VD1 can inhibit >80% of EGFP-TnR: β3 complex formation whereas VD1A50I has only a 10% effect that is not concentration-dependent (Fig. 4A). Because VD1A50I binds as well as VD1 to β3 (Fig. 2A,B), we conclude that the inhibitory effect of VD1 cannot be the result of VD1 competing with TnR for binding sites on β3. By default, the inhibitory effect of VD1 on Tn and TnR binding to β3 must result from binding of VD1 to TnR.

The biphasic curve for VD1 inhibition of the β3:EGFP-TnR interaction and the fact that there are 11 potential VD1 binding sites (VBSs) on TnR [Gingras et al., 2005] prompted us to examine the concentration dependence for VD1 binding to EGFP-TnR. We found that 6His VD1 can pull down 100% of the EGFP-TnR that is competent to bind β3 (i.e. ~70%) with a half maximum effect at 0.25 μM VD1, whereas ~5 μM VD1 is required to inhibit 50% of the maximal TnR: β3 interaction (Fig. 4A,B). Inspection of the dose-response curves at low concentration of VD1 (Fig. 4B), shows little inhibitory effect of VD1 at concentrations that pull down nearly all of the binding-competent TnR, i.e. 0.5–1 μM. The data suggest that a high affinity interaction directs the initial binding of VD1 to TnR, but that occupancy of lower affinity sites is required for VD1 inhibition of Tn and TnR binding to β3. The presence of 11 cryptic VD1 binding

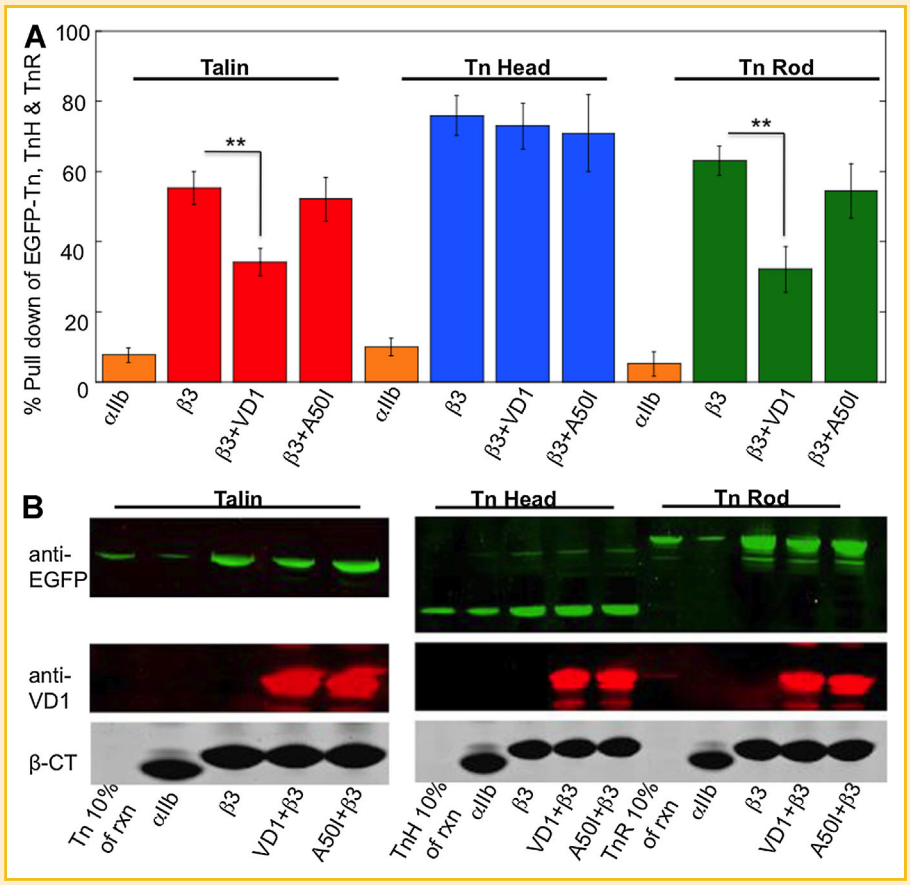


**Fig. 3.** VD1, but not VD1A50I, inhibits binding of TnR and Tn, but not TnH to the β3 cytoplasmic tail. (A) The cytoplasmic tail of β3 or αIIb integrin coupled to NTA beads was used to pull down EGFP-tagged Tn constructs from cell lysates in the absence or presence of VD1 (wt or A50I). αIIb cytoplasmic tail coupled to NTA beads showed minimal binding to the talin constructs. Inhibition of TnR: β3 complex by VD1 depends on interaction of VD1 with TnR because VD1A50I has no effect. Data represent means ± SEM (n = 5). **, $P < 0.01$. (B) Proteins pulled down by the β3-NTA beads were separated on 4–12% SDS-PAGE and analyzed by Western blotting. EGFP-Tn constructs and VD1 (wt or A50I) were detected by blotting with anti-EGFP and VinG-11 antibody, respectively. The low molecular weight β3 integrin cytoplasmic tail was detected by staining that portion of the gel with Coomassie-formaldehyde.

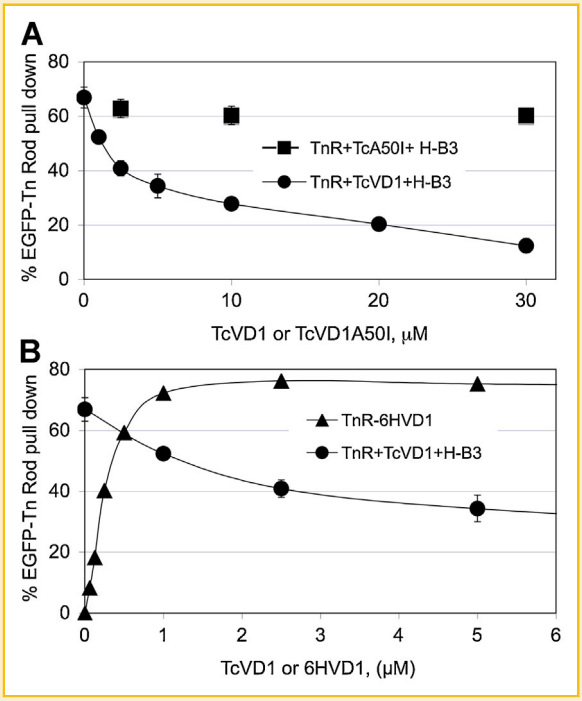


**Fig. 4.** Distinct concentration dependencies for VD1 inhibition of EGFP-TnR-β3 integrin interaction versus binding of VD1 to EGFP-TnR. (A) The effect of VD1 concentration on EGFP-Tn Rod interaction with β3-NTA beads was measured using the supernatant depletion assay. VD1 at 5 μM inhibited ~50% of EGFP-TnR binding to β3 tail (filled circles). VD1A50I did not show concentration-dependent inhibition of the TnR- β3 interaction (filled squares) and had only a small inhibitory effect (n = 2). (B) Data for the 1–6 μM of (A) plotted with the concentration-dependence for binding of 6HisVD1 to EGFP-TnR (filled triangles) shows that 1 μM VD1 is sufficient to pull down ~75% TnR (i.e., 100% of TnR that is competent to bind to β3) but results in only ~20% inhibition of the TnR- β3 interaction.

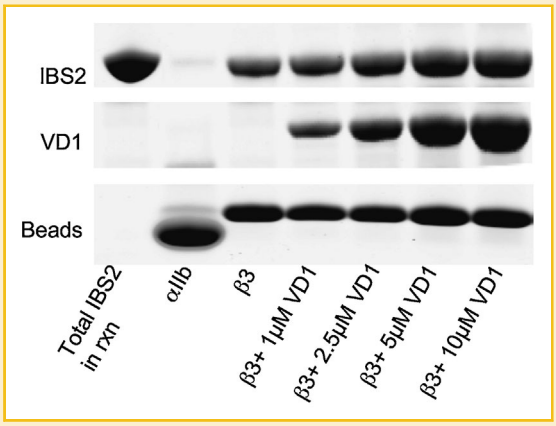


**Fig. 5.** Effect of VD1 on the IBS2 binding to β3 integrin cytoplasmic tail. SDS PAGE analysis of IBS2 (2.5 μM) interaction with β3-NTA beads (11 μM) in presence of increasing concentrations of VD1 over a period of 16–18 h at 37 °C.

sites on TnR [Gingras et al., 2005] provides opportunity for more than 1 VD1 to bind to TnR.

## DOES VD1 ALTER THE IBS2 DOMAIN INTERACTION WITH β3 INTEGRIN TAIL?

The integrin binding site (IBS2) is a well-established site in TnR that also has a vinculin binding site in the Helix 50 [Rodius et al., 2008 Gingras et al., 2009; Yogesha et al., 2012]. This domain could bind well to both β3CT and VD1, so it was quite possible that binding of VD1 to IBS2 might perturb its binding to β3 tail. To test this idea we examined the effect of incubating increasing concentrations of VD1 on the binding of IBS2 domain to β3CT coupled to NTA beads. The results show that even at high concentrations of VD1, the IBS2: β3CT binding was not effected (Fig. 5). Mutant VD1A50I too had no inhibitory effect on the amount of β3CT:IBS2 complex formed (data not shown). This experiment clearly shows that under in vitro conditions, VD1 does not inhibit IBS2 domain binding to β3CT.

## SECOND INTEGRIN BINDING SITE IN TnR, IBS3

The in vitro biochemical assays show that VD1 inhibition of binding of TnR to β3CT (Fig. 3) is not through the IBS2 domain in TnR (Fig. 5). There are 11 known VBSs on TnR, so we speculated that VD1 could be binding to some other VBS (other than the one in IBS2 domain) and interfering with the β3CT binding. We examined the most probable candidate, R1-R3 domain [Papagrigoriou et al., 2004; Goult et al., 2013], a VBS rich region containing 5 vinculin binding sequences that binds well to VD1 [Fillingham et al., 2005]. We evaluated using in vitro binding assay the ability of β3CT to bind TnR 482-911. Data indicates that TnR 482-911 showed low, but specific binding to β3CT (Fig. 6A) as further supported by the binding data using β3 mutants; β3 Y/A and β3 FF/AA [Anthis et al., 2010]. This putative integrin-binding site could have been missed in earlier mapping studies done, when the tertiary domains of TnR were unknown. We evaluated the role of TnR 482-911 further using the competition inhibition assay. Results show that in presence of increasing VD1 concentration, the binding of TnR 482-911 to β3CT (Fig. 6B) was almost completely inhibited. This inhibition was specific and dependent on VD1 association with talin rod, as the VD1A50I mutant showed no significant inhibition of TnR 482-911 binding to β3CT (Fig. 6C). Binding of VD1 to this potential IBS3 region in TnR might be subsequently interfering with β3CT binding. However, by itself TnR 482-911 was a weak and inconsistent inhibitor of TnR binding to β3 (~20% inhibition at 20 μM TnR 482-911, data not shown). Further experiments are needed to verify the role of IBS3 (aa 482-911) in regulating TnR interaction with β3CT in presence of VD1.

## HOW DOES VINCULIN ACTIVATE INTEGRIN IN CELLS?

Our in vitro results show inhibitory effect of VD1 on interaction of TnR and Tn with β3. However on the contrary, a recent study shows that activated vinculin activates αIIbβ3 in a manner dependent on talin [Ohmori et al., 2010]. To investigate this further, we used the PAC1 binding integrin activation assay (Fig. 7A,B). CHOA5 cells were transfected with talin and vinculin constructs, the talin binding (VhA50I) and autoinhibition mutants of vinculin (V-T12, V-T12A50I). Analysis of the FACS data shows that CHO cells transfected with TnH and Tn constructs showed enhanced PAC1

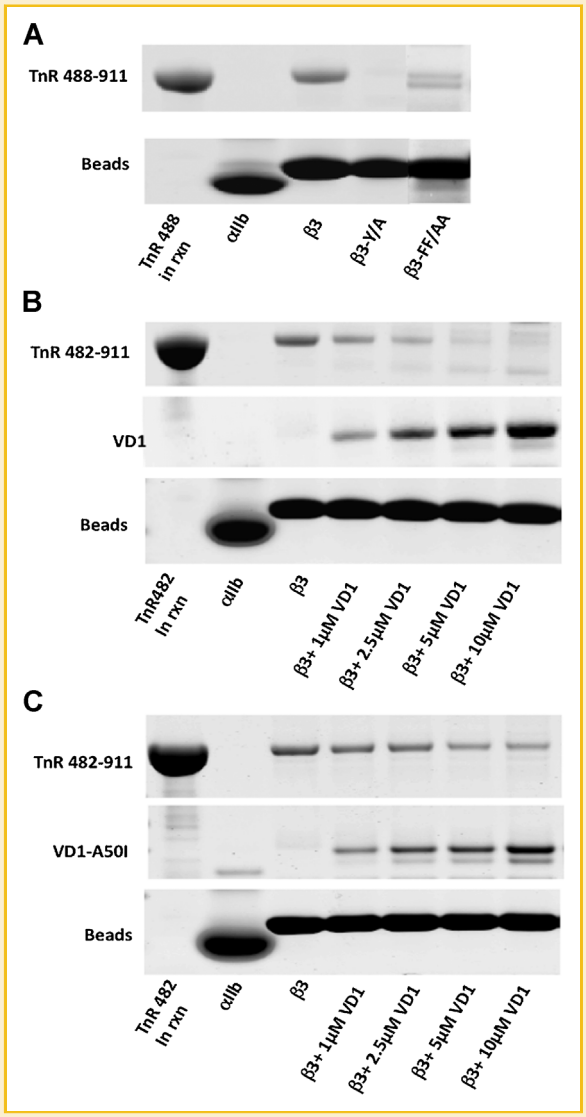


**Fig. 6.** TnR 482–911 binds specifically to β3CT and binding is inhibited by VD1. (A) β3CT wild type, β3CT mutants or αIIb-CT coupled to NTA beads were used to pull down purified and TEV cleaved TnR482–911 domain (1 μM) overnight at 37 °C. The results were analyzed on 4–12% SDS-PAGE; first lane shows total TnR482–911 in reaction and the subsequent lanes show the differential binding of TnR482–911 with αIIb, β3, and its mutants. (B, C) Interaction of 2.5 μM TnR482–911 with β3CT-NTA beads (11 μM) in presence of increasing concentrations of VD1 and VD1A50I, incubated overnight at 37 °C and analyzed by SDS PAGE.

binding and that TnH was a better activator compared to the FL Tn (Fig. 7A,B). TnR however, had absolutely no effect on PAC1 binding. Earlier studies done using the IBS2 domain of TnR have also suggested that TnR is not involved in integrin activation [Tremuth et al., 2004]. FL vinculin and A50I mutants showed no integrin activation, while the Vh and V-T12 showed enhanced PAC-1 binding, as also previously reported [Ohmori et al., 2010]. Activated vinculin shows talin dependent integrin activation as the A50I VD1, like TnR, showed no enhanced PAC1 binding. Based on these observations we reasoned that activated vinculin might mediate talin-dependent integrin activation by displacing or preventing the non-productive interaction of TnR with the β3 subunit, thereby releasing that β3 to interact with TnH and enhancing integrin activation.

## DISCUSSION

In this study we employed in vitro biochemistry together with experiments in mammalian cells to achieve some mechanistic understanding of how vinculin enhances integrin-mediated cell adhesion. Vinculin is possibly involved in strengthening the talin-β3 integrin interaction by either: (1) binding directly to the β3 cytoplasmic tail and further strengthening talin interaction with integrins or (2) by binding to talin and regulating its binding to β3CT. Although the results obtained were more complex than expected, several novel observations were made.

### VINCULIN: A DIRECT LIGAND FOR INTEGRIN CYTOPLASMIC TAILS

Over the last decade, approximately 40 proteins that bind to integrin cytoplasmic tails have been described [Legate and Fassler, 2009]. Some of these, including talin [Tadokoro et al., 2003], filamin, kindlins, and Zasp regulate inside-out integrin activation, whereas others such as src, are not required for inside-out integrin activation but are themselves activated by integrin to regulate outside-in integrin–dependent pathways [Arias-Salgado et al., 2003]. However, for many of the reported interactions, including vinculin, there is not a demonstrated function and this remains an important question for future studies. To address how VD1 activates integrin αIIbβ3 in cells in a talin-dependent manner, we turned to a previously established in vitro system. We found a specific, direct, and differential interaction of vinculin domain, VD1 with β3, β1 A, and β1D integrin cytoplasmic tails. It is possible that this novel interaction might strengthen integrin-based transmembrane adhesion structures through talin-independent linkage to the actin cytoskeleton.

### VINCULIN BINDING TO Tn/TnR DOWNREGULATES THE INTERACTION OF TN WITH β3CT IN VITRO

Several reports have shown that activated vinculin stimulates co-localization of talin with activated integrin in cells [Cohen et al., 2005; Humphries et al., 2007; Banno et al., 2012]. In light of these results, we expected to find that VD1 promotes association of talin with integrin β3CT in vitro. In contrast to this expectation, we found that VD1 inhibits TnR binding to β3, while having no effect on binding of TnH to β3. The inhibition is not steric and is talin-dependent as proven by taking mutant VD1A50I as control. Taken together, the observations suggest that, in vitro, binding of VD1 to TnR causes a conformational change in TnR domain and interferes with the accessibility of its integrin binding site to β3CT. The only well defined integrin binding site (IBS) in TnR is the IBS2 domain [Rodius et al., 2008 Gingras et al., 2009] that also contain a VBS (VBS50). However, our in vitro competitive inhibition assay result shows that in the context of full length TnR, the inhibition of TnR binding to β3 is not mediated through VD1 binding to IBS2. This could possibly be due to restrained accessibility of VBS50 in context of the TnR molecule. The results are supported by a recent study of

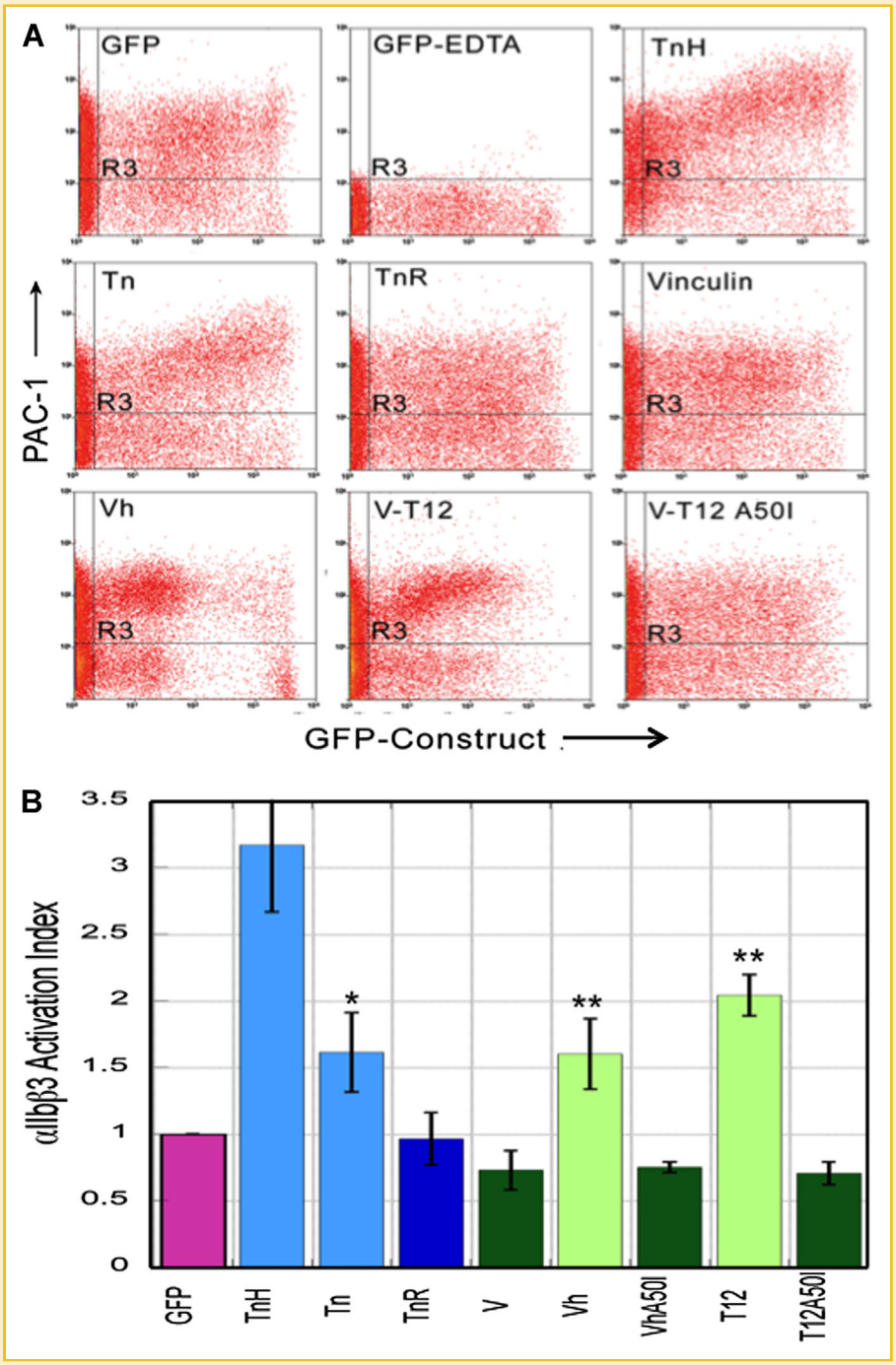


**Fig. 7.** Activated vinculin and talin constructs except TnR enhances integrin activation in CHOA5 cells. (A) Representative flow cytometry results for CHO cells expressing αIIbβ3, transfected with EGFP-tagged talin or vinculin constructs, as specified. Live cells were stained with PAC1 antibody to detect activated αIIbβ3 or A2A9 to detect total cell surface αIIbβ3. Controls, calculation of activation index, and details of the protocol are described in Materials and Methods (B) Bar graph represents the data for different constructs normalized to PAC1 binding on cells expressing EGFP only (activation index = 1). Error bars are mean ± SEM (n = 4). *, $P = 0.06$; **, $P < 0.05$.

VBS50 domain in complex with vinculin [Yogesha et al., 2012] that shows that the affinity of VBS50 for vinculin is about 30 times less than other VBSs in TnR. The VBS50 is buried in the groove and a mechanical tension like integrin binding to TnR, is needed to destabilize IBS2 and to allow it to bind to vinculin.

Interestingly, we found a new integrin-binding site in a well-defined VBS rich domain aa 482-911 in TnR [Papagrigoriou et al., 2004 Fillingham et al., 2005; Gingras et al., 2005]. Competitive inhibition assay show that VD1 binding to TnR 482-911 domain inhibited its binding to β3CT and that the inhibitory effect was talin

rod dependent. However, unlike the purified IBS2 domain, the purified TnR482-911 domain does not compete with TnR for binding to β3. We reasoned that this could be due to the autoinhibitory conformation of Tn molecule, as suggested by earlier studies [Johnson and Craig, 1994 Goksoy et al., 2008]. The TnR 482-911 domain is probably not accessible for interaction with β3CT as also suggested by studies done using NMR [Banno et al., 2012] that show that TnR (aa 482-787) domain is involved in inter-domain interaction with TnH. However in presence of VD1, we speculate that VD1 binding to TnR 482-911 domain causes conformational changes in the TnR that interferes with its ability to interact with integrin β3 cytoplasmic tail.

## VINCULIN'S FUNCTION IN INTEGRIN ACTIVATION

Compelling evidence shows that vinculin enhances talin-mediated integrin activation in cells [Nolz et al., 2007; Ohmori et al., 2010], but the mechanisms are not yet clear. Our PAC1 binding assay results using vinculin constructs are in consent with these earlier findings. Tn and TnH constructs show enhanced PAC1 binding, but interestingly TnR that has well-defined IBS2, shows no enhanced PAC1 binding. Earlier studies using CHOA5 cells, had shown that a fragment of TnR fragment G (aa 1984-2344), that contains most of the IBS2 [Gingras et al., 2009] and also binds β3CT, had no effect on basal αIIbβ3 activation [Tremuth et al., 2004]. Results from our biochemical studies too suggest, that VD1 binding to IBS2 domain does not interfere with its binding to β3CT. Our observations from in vitro and PAC1 binding assays led us to propose a hypothesis, that binding of TnR to β3 acts as a brake on integrin activation and that VD1 interferes with this process (Fig. 8). According to the hypothesis, VD1 binding to VBS rich region in TnR (aa 482-911) induces conformational changes in TnR that interferes with TnR interaction with integrin β3CT. Thus activated vinculin stimulates integrin activation by preventing a non-productive interaction of TnR with integrin β3 and making β3 CT available for interaction with TnH. In addition to this, direct binding of VD1 to β3 could also have a role in integrin activation by recruiting more Tn molecules to integrin tails and also enhancing integrin clustering in the process. This idea is consistent with the findings that expression of VD1 or Vh in cells leads to hypertrophied FA growth and increased residence time of talin and activated vinculin in the FA [Cohen et al., 2006; Humphries et al., 2007]. It is possible that vinculin has a dual role, one involving its effects on the Tn: β3 interaction and one depending on direct interaction of Vh/VD1 with β3 (Fig. 8).

In summary, we present the first evidence for a direct interaction between integrin cytoplasmic tails and vinculin, VD1. We also document an inhibitory effect of VD1 on Tn and TnR binding to integrin cytoplasmic tails in vitro and show that this inhibition is dependent on VD1 binding to TnR. We further confirm the stimulatory effect of activated vinculin constructs on αIIbβ3 integrin activation in CHOA5 cells, and describe a VD1-regulated, second integrin binding site in TnR. The new observations and results presented in this paper provide a basis for further investigation of the mechanisms by which vinculin stimulates integrin activation in cells.

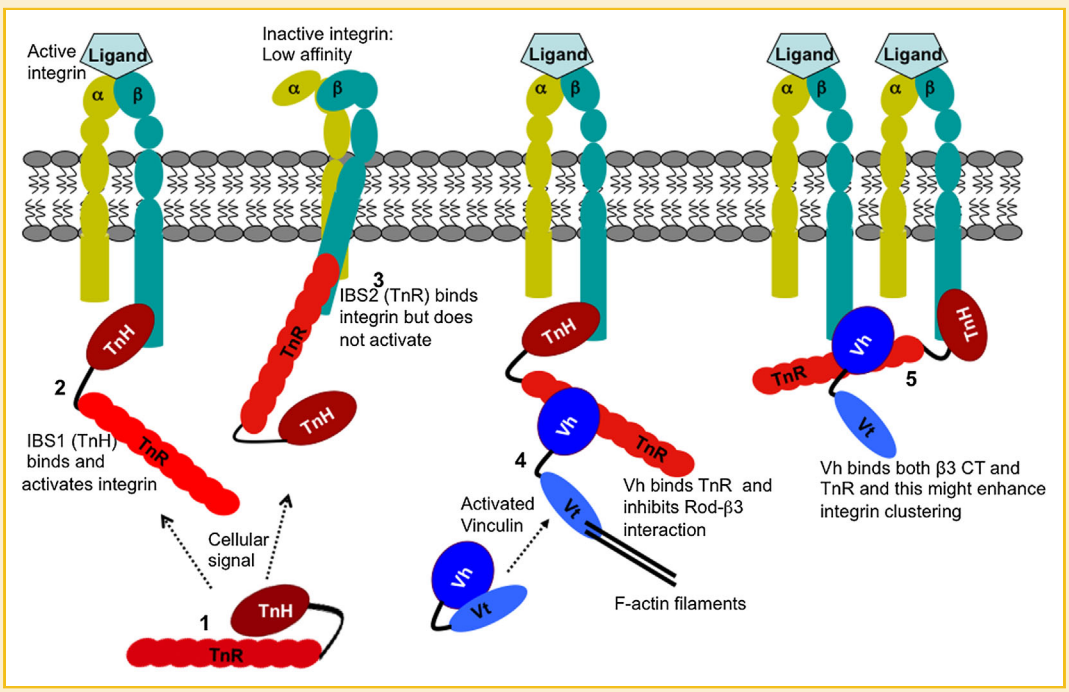


**Fig. 8.** Model for the role of vinculin in inducing the talin mediated integrin activation. Talin undergoes a conformational change induced by a cellular signal that releases its autoinhibitory state [Goksoy et al., 2008] in the FAs. Both talin head (TnH) and talin rod (TnR) interact with the β3CT (shown in cyan), but only TnH induces integrin activation by unclasping the α & β heterodimer. Vinculin too is released from its autoinhibitory state at the site of focal adhesion by binding to F-actin and talin [Bakolitsa et al., 1999; Chen et al., 2006]. The head (Vh) domain of activated vinculin interacts with TnR and β3CT and the tail (Vt) domain interacts with F-actin filaments. Binding of Vh to TnR interferes with its binding to β3CT and the direct binding of Vh to β3CT might enhance integrin clustering.

## ACKNOWLEDGEMENTS

This research was supported by NIH grant (GM41605) to Susan W. Craig and was performed in the laboratory of Susan Craig in the Biological Chemistry department at Johns Hopkins School of Medicine.

## REFERENCES

Abrams C, Deng YJ, Steiner B, O'Toole T, Shattil SJ. 1994. Determinants of specificity of a baculovirus-expressed antibody Fab fragment that binds selectively to the activated form of integrin alpha IIb beta 3. J Biol Chem 269:18781–18788.

Anthis NJ, Wegener KL, Critchley DR, Campbell ID. 2010. Structural diversity in integrin/talin interactions. Structure 18:1654–1666.

Anthis NJ, Wegener KL, Ye F, Kim C, Goult BT, Lowe ED, Vakonakis I, Bate N, Critchley DR, Ginsberg MH, Campbell ID. 2009. The structure of an integrin/talin complex reveals the basis of inside-out signal transduction. Embo J 28:3623–3632.

Arias-Salgado EG, Lizano S, Sarkar S, Brugge JS, Ginsberg MH, Shattil SJ. 2003. Src kinase activation by direct interaction with the integrin beta cytoplasmic domain. Proc Natl Acad Sci USA 100:13298–13302.

Bakolitsa C, de Pereda JM, Bagshaw CR, Critchley DR, Liddington RC. 1999. Crystal structure of the vinculin tail suggests a pathway for activation. Cell 99:603–613.

Banno A, Goult BT, Lee H, Bate N, Critchley DR, Ginsberg MH. 2012. Subcellular localization of talin is regulated by inter-domain interactions. J Biol Chem 287:13799–13812.

Bennett JS, Hoxie JA, Leitman SF, Vilaire G, Cines DB. 1983. Inhibition of fibrinogen binding to stimulated human platelets by a monoclonal antibody. Proc Natl Acad Sci USA 80:2417–2421.

Bozyczko D, Decker C, Muschler J, Horwitz AF. 1989. Integrin on developing and adult skeletal muscle. Exp Cell Res 183:72–91.

Bunch TA. 2010. Integrin alphaIIbbeta3 activation in Chinese hamster ovary cells and platelets increases clustering rather than affinity. J Biol Chem 285:1841–1849.

Calderwood DA, Zent R, Grant R, Rees DJ, Hynes RO, Ginsberg MH. 1999. The Talin head domain binds to integrin beta subunit cytoplasmic tails and regulates integrin activation. J Biol Chem 274:28071–28074.

Chen H, Choudhury DM, Craig SW. 2006. Coincidence of actin filaments and talin is required to activate vinculin. J Biol Chem 281(52):40389–40398. DOI: 10.1074/jbc.M607324200. Epub 2006 Oct 29.

Chen H, Cohen DM, Choudhury DM, Kioka N, Craig SW. 2005. Spatial distribution and functional significance of activated vinculin in living cells. J Cell Biol 169:459–470.

Cohen DM, Chen H, Johnson RP, Choudhury B, Craig SW. 2005. Two distinct head-tail interfaces cooperate to suppress activation of vinculin by talin. J Biol Chem 280:109–117.

Cohen DM, Kutscher B, Chen H, Murphy DB, Craig SW. 2006. A conformational switch in vinculin drives formation and dynamics of a talin-Vinculin complex at focal adhesions. J Biol Chem 281:16006–16015.

Fillingham I, Gingras AR, Papagrigoriou E, Patel B, Emsley J, Critchley DR, Roberts GC, Barsukov IL. 2005. A vinculin binding domain from the talin rod unfolds to form a complex with the vinculin head. Structure (Camb) 13: 65–74.

Gallant ND, Michael KE, Garcia AJ. 2005. Cell adhesion strengthening: Contributions of adhesive area, integrin binding, and focal adhesion assembly. Mol Biol Cell 16:4329–4340.

Gingras AR, Ziegler WH, Bobkov AA, Joyce MG, Fasci D, Himmel M, Rothemund S, Ritter A, Grossmann JG, Patel B, Bate N, Goult BT, Emsley J, Barsukov IL, Roberts GC, Liddington RC, Ginsberg MH, Critchley DR. 2009. Structural determinants of integrin binding to the talin rod. J Biol Chem 284:8866–8876.

Gingras AR, Ziegler WH, Frank R, Barsukov IL, Roberts GC, Critchley DR, Emsley J. 2005. Mapping and consensus sequence identification for multiple vinculin binding sites within the talin rod. J Biol Chem 280:37217–37224.

Goksoy E, Ma YQ, Wang X, Kong X, Perera D, Plow EF, Qin J. 2008. Structural basis for the autoinhibition of talin in regulating integrin activation. Mol Cell 31:124–133.

Goult BT, Zacharchenko T, Bate N, Tsang R, Hey F, Gingras AR, Elliott PR, Roberts GC, Ballestrem C, Critchley DR, Barsukov IL. 2013. RIAM and vinculin binding to talin are mutually exclusive and regulate adhesion assembly and turnover. J Biol Chem 288(12):8238–8249. DOI:10.1074/jbc.M112.438119. Epub 2013 Feb 6.

Humphries JD, Wang P, Streuli C, Geiger B, Humphries MJ, Ballestrem C. 2007. Vinculin controls focal adhesion formation by direct interactions with talin and actin. J Cell Biol 179:1043–1057.

Hynes RO. 2002. Integrins: Bidirectional, allosteric signaling machines. Cell 110:673–687.

Izard T, Evans G, Borgon RA, Rush CL, Bricogne G, Bois PR. 2004. Vinculin activation by talin through helical bundle conversion. Nature 427:171–175.

Johnson RP, Craig SW. 1994. An intramolecular association between the head and tail domains of vinculin modulates talin binding. J Biol Chem 269:12611–12619.

Johnson RP, Craig SW. 1995. F-actin binding site masked by the intramolecular association of vinculin head and tail domains. Nature 373:261–264.

Lad Y, Harburger DS, Calderwood DA. 2007. Integrin cytoskeletal interactions. Methods Enzymol 426:69–84.

Legate KR, Fassler R. 2009. Mechanisms that regulate adaptor binding to beta-integrin cytoplasmic tails. J Cell Sci 122:187–198.

Leisner TM, Yuan W, DeNofrio JC, Liu J, Parise LV. 2007. Tickling the tails: Cytoplasmic domain proteins that regulate integrin alphaIIbbeta3 activation. Curr Opin Hematol 14(3):255–261.

McCann RO, Craig SW. 1997. The I/LWEQ Module: A conserved sequence that signifies F-actin binding in functionally diverse proteins from yeast to mammals. Proc Natl Acad Sci USA 94:5679–5684.

Moes M, Rodius S, Coleman SJ, Monkley SJ, Goormaghtigh E, Tremuth L, Kox C, van der Holst PP, Critchley DR, Kieffer N. 2007. The integrin binding site 2 (IBS2) in the talin rod domain is essential for linking integrin beta subunits to the cytoskeleton. J Biol Chem 282:17280–17288.

Ni H, Li A, Simonsen N, Wilkins JA. 1998. Integrin activation by dithiothreitol or Mn2+ induces a ligand-occupied conformation and exposure of a novel NH2-terminal regulatory site on the beta1 integrin chain. J Biol Chem 273:7981–7987.

Nolz JC, Medeiros RB, Mitchell JS, Zhu P, Freedman BD, Shimizu Y, Billadeau DD. 2007. WAVE2 regulates high-affinity integrin binding by recruiting vinculin and talin to the immunological synapse. Mol Cell Biol 27:5986–6000.

Ohmori T, Kashiwakura Y, Ishiwata A, Madoiwa S, Mimuro J, Honda S, Miyata T, Sakata Y. 2010. Vinculin activates inside-out signaling of integrin alphaIIbbeta3 in Chinese hamster ovary cells. Biochem Biophys Res Commun 400:323–328.

Papagrigoriou E, Gingras AR, Barsukov IL, Bate N, Fillingham IJ, Patel B, Frank R, Ziegler WH, Roberts GC, Critchley DR, Emsley J. 2004. Activation of a vinculin-binding site in the talin rod involves rearrangement of a five-helix bundle. Embo J 23:2942–2951.

Pfaff M, Liu S, Erle DJ, Ginsberg MH. 1998. Integrin beta cytoplasmic domains differentially bind to cytoskeletal proteins. J Biol Chem 273:6104–6109.

Priddle H, Hemmings L, Monkley S, Woods A, Patel B, Sutton D, Dunn GA, Zicha D, Critchley DR. 1998. Disruption of the talin gene compromises focal

adhesion assembly in undifferentiated but not differentiated embryonic stem cells. J Cell Biol 142:1121–1133.

Rodius S, Chaloin O, Moes M, Schaffner-Reckinger E, Landrieu I, Lippens G, Lin M, Zhang J, Kieffer N. 2008. The talin rod IBS2 alpha-helix interacts with the beta3 integrin cytoplasmic tail membrane-proximal helix by establishing charge complementary salt bridges. J Biol Chem 283:24212–24223.

Smith SJ, McCann RO. 2007. A C-terminal dimerization motif is required for focal adhesion targeting of Talin1 and the interaction of the Talin1 I/LWEQ module with F-actin. Biochemistry 46:10886–10898.

Tadokoro S, Shattil SJ, Eto K, Tai V, Liddington RC, de Pereda JM, Ginsberg MH, Calderwood DA. 2003. Talin binding to integrin beta tails: A final common step in integrin activation. Science 302:103–106.

Tremuth L, Kreis S, Melchior C, Hoebeke J, Ronde P, Plancon S, Takeda K, Kieffer N. 2004. A fluorescence cell biology approach to map the second integrin-binding site of talin to a 130-amino acid sequence within the rod domain. J Biol Chem 279:22258–22266.

Ulmer TS, Yaspan B, Ginsberg MH, Campbell ID. 2001. NMR analysis of structure and dynamics of the cytosolic tails of integrin alpha IIb beta 3 in aqueous solution. Biochemistry 40:7498–7508.

Wegener KL, Partridge AW, Han J, Pickford AR, Liddington RC, Ginsberg MH, Campbell ID. 2007. Structural basis of integrin activation by talin. Cell 128:171–182.

Xu W, Coll JL, Adamson ED. 1998. Rescue of the mutant phenotype by reexpression of full-length vinculin in null F9 cells; effects on cell locomotion by domain deleted vinculin. J Cell Sci 111:1535–1544.

Yogesha SD, Rangarajan ES, Vonrhein C, Bricogne G, Izard T. 2012. Crystal structure of vinculin in complex with vinculin binding site 50 (VBS50), the integrin binding site 2 (IBS2) of talin. Protein Sci 21:583–588.

Zaffran Y, Meyer SC, Negrescu E, Reddy KB, Fox JE. 2000. Signaling across the platelet adhesion receptor glycoprotein Ib-IX induces alpha IIbbeta 3 activation both in platelets and a transfected Chinese hamster ovary cell system. J Biol Chem 275:16779–16787.

## SUPPORTING INFORMATION

Additional supporting information may be found in the online version of this article at the publisher's web-site.